

4 From link dynamics to path lifetime and packet-length 5 optimization in MANETs

6 Xianren Wu · Hamid R. Sadjadpour ·
7 J. J. Garcia-Luna-Aceves

8
9 © Springer Science+Business Media, LLC 2007

10 **Abstract** We present an analytical framework and sta-
11 tistical models to accurately characterize the lifetime of a
12 wireless link and multi-hop paths in mobile ad hoc net-
13 works (MANET). We show that the lifetimes of links and
14 paths can be computed through a two-state Markov model.
15 We also show that the analytical solution follows closely
16 the results obtained through discrete-event simulations for
17 two mobility models, namely, random direction and ran-
18 dom waypoint mobility models. We apply these models to
19 study practical implications of link lifetime on routing
20 protocols. First, we compute optimal packet lengths as a
21 function of mobility, and show that significant throughput
22 improvements can be attained by adapting packet lengths
23 to the mobility of nodes in a MANET. Second, we show
24 how the caching strategy of on-demand routing protocols
25 can benefit from considering the link lifetimes in a
26 MANET. Finally, we summarize all the analytical results
27 into a comprehensive performance analysis on throughput,
28 delay and storage.

29
30 **Keywords** Link dynamics · Analytical mobility
31 modeling · Path lifetime · Markov model · Optimal
32 information segmentation
33

A1 X. Wu (✉) · H. R. Sadjadpour · J. J. Garcia-Luna-Aceves
A2 University of California at Santa Cruz, Santa Cruz,
A3 CA 95064, USA
A4 e-mail: wuxr@soe.ucsc.edu

A5
A6 H. R. Sadjadpour
A7 e-mail: hamid@soe.ucsc.edu

A8 J. J. Garcia-Luna-Aceves
A9 Palo Alto Research Center, 3333 Coyote Hill Road, Palo Alto,
A10 CA 94304, USA
A11 e-mail: jj@soe.ucsc.edu

1 Introduction 34

The communication protocols of mobile ad hoc networks (MANET) must cope with frequent changes in topology due to node mobility and the characteristics of radio channels. From the standpoint of medium access control (MAC) and routing, node mobility and changes in the state of radio channels translate into changes in the state of the wireless links established among nodes, where typically a wireless link is assumed to exist when two nodes are able to decode each other's transmissions.

The motivation for this paper is that, while the behavior of wireless links is critical to the performance of MAC and routing protocols operating in a MANET, no analytical model exists today that accurately characterizes the lifetime of wireless links, and the paths they form from sources to destinations, as a function of node mobility. As a result, the performance of MAC and routing protocols in MANETs have been analyzed through simulations, and analytical modeling of channel access and routing protocols for MANETs have not accounted for the temporal nature of MANET links and paths. For example, the few analytical models that have been developed for channel access protocols operating in multihop ad hoc networks have either assumed static topologies (e.g., [1]) or focused on the immediate neighborhood of a node, such that nodes remain neighbors for the duration of their exchanges (e.g., [2]). Similarly, most studies of routing-protocol performance have relied exclusively on simulations, or had to use limited models of link availability (e.g., [3]) to address the dynamics of paths impacting routing protocols (e.g., [4]).

This paper provides the most accurate analytical model of link and path behavior in MANETs to date, and

68 characterizes the behavior of links and paths as a function
69 of node mobility. The importance of this model is twofold.
70 First, it enables the investigation of many questions
71 regarding fundamental tradeoffs in throughput, delay and
72 storage requirements in MANETs, as well as the relation-
73 ship between many crosslayer-design choices (e.g.,
74 information packet length) and network dynamics (e.g.,
75 how long links last in a MANET). Second, it enables the
76 development of new analytical models for channel access,
77 clustering and routing schemes by allowing such models to
78 use link lifetime expressions that are accurate with respect
79 to simulations based on widely used mobility models.

80 Recently, Samar and Wicker [5, 6] pioneered the ana-
81 lytical evaluation of link dynamics, and provided new
82 insight on the importance of an analytical formulation of
83 link dynamics in the optimization of the protocol design.
84 However, Samar and Wicker assumed that communicating
85 nodes maintain constant speed and direction in order to
86 evaluate the distribution of link lifetime. This simplifica-
87 tion overlooks the case in which either one of the
88 communicating nodes changes its speed or direction while
89 the nodes are in transmission range of each other. As a
90 result, the results predicted by Samar and Wicker's model
91 could deviate from reality greatly, being overly conserva-
92 tive and underestimating the distribution of link lifetime
93 [5, 6], especially when the ratio R/v between the radius of
94 the communication range R to the node speed v becomes
95 large, such that nodes are likely to change their velocity
96 and direction during an exchange.

97 The contribution of this paper is to provide a two-state
98 Markov model that better describes the mobility patterns of
99 communicating nodes. Section 2 describes the network and
100 mobility models used to characterize link and path
101 behavior. Section 3 describes the proposed analytical
102 framework and presents our results on link lifetime, and
103 Sect. 4 extends these results to path dynamics. Our
104 approach is based on a two-state Markovian model that
105 reflects the movements of nodes inside the circle of
106 transmission range and builds an analytical framework to
107 accurately evaluate the distribution of link lifetime.

108 Our model subsumes the model of Samar and Wicker
109 [5, 6] as a special case, and provides a more accurate
110 characterization of the statistics of link lifetime. Section 5
111 illustrates the accuracy of our analytical model by com-
112 paring the analytical results against simulations based on
113 the random direction mobility model (RDMM) and the
114 random waypoint mobility (RWP) model.

115 Sections 6 and 7 illustrate how our model can be applied
116 to practical problems in MANETs. Section 6 applies our
117 analytical framework to optimal segmentation (information
118 packet length) of information streams. Our results reveal
119 that packet lengths should be designed to be linearly pro-
120 portional to the ratio R/v , and show that the optimal packet

length for a given K -hop path should be designed to be
 $R/(vK)$. Section 7 discusses improving packet caching
policies in on-demand routing protocols by taking advan-
tage of the characterization of link and path lifetimes. A
comprehensive coverage of throughput, delay and storage
requirement is then followed in Sect. 8. Part of the material
in this paper was presented in [7], for a particular mobility
model (RDMM) and restricted mobility of nodes. This
paper considers a more general random mobility model,
extensions to path dynamics, and unrestricted node
mobility.

2 System model

Consistent with several prior analytical models of MANETs
[8–10], we consider a square network of size
 $L \times L$ in which n nodes are initially randomly deployed.
The movement of each node is unrestricted, i.e., the trajec-
tories of nodes can be anywhere in the network. The model of
node mobility falls into the general category of random trip
mobility model [11], where nodes' movement can be
described by a continuous-time stochastic process and the
movement of nodes can be divided into a chain of trips.

Communication between two nodes is allowed only
when the distance between them is less than or equal to R
and can be performed reliably. Communication zone of a
given node consisting of the circle of radius R satisfies the
minimum SINR (signal to interference plus noise ratio)
requirement with certain outage probability in the wireless
fading environment.

A typical communication session between two nodes
involves several control and data packet transmissions.
Depending on the protocol, nodes may be required to
transmit beacons to their neighbors to synchronize their
clocks for a variety of reasons (e.g., power management,
frequency hopping). Nodes can find out about each other's
presence by means of such beacons, or by the reception of
other types of signaling packets (e.g., HELLO messages).
Once a transmitter knows about the existence of a receiver,
it can send data packets, which are typically acknowledged
one by one, and the MAC protocol attempts to reduce or
avoid those cases in which more than one transmitter sends
data packets around a given receiver, which typically
causes the loss of all such packets at the receiver. To
simplify our modeling of link lifetime, we assume that the
proper mechanisms are in place for neighboring nodes to
find each other, and that all transmissions of data packets
are successful, as long as they do not last beyond the
lifetime of the wireless link between transmitter and
receiver. Relaxing this simplifying assumption is the sub-
ject of future work, as it involves the modeling of explicit
medium access control schemes (e.g., [1]).

171 **3 Link lifetime**

172 A bidirectional link exists between two nodes if they are
 173 within communication range of each other. In this paper,
 174 we do not consider unidirectional links, given that the vast
 175 majority of channel access and routing protocols use only
 176 bidirectional links for their operation. Hence, we will refer
 177 to bidirectional links simply as links for the rest of this
 178 paper.

179 The wireless link between nodes m_a and m_b is broken
 180 when the distance between nodes m_a and m_b is greater than
 181 R . When a data packet starts at time t_1 , the positions of
 182 node m_b could be anywhere inside the communication
 183 circle defined by the transmission range of m_a and is
 184 assumed as uniformly distributed.¹

185 Let B (bits/s) be the transmission rate of a data packet,
 186 L_p be the length of the data packet, and $t_1 + T_L$ denote the
 187 moment that node m_b is moving out of the communication
 188 circle. A data packet can be successfully transferred only if
 189 nodes m_a and m_b stay within their communication range
 190 during the whole communication session of the data
 191 packet, that is,

$$L_p/B \leq T_L \tag{1}$$

193 where T_L is the link lifetime (LLT) denoting the maximum
 194 possible data transfer duration. Statistically, T_L specifies
 195 the distribution of residence time that measures the
 196 duration of the time, for node m_b , starting from a random
 197 point inside the communication circle with equal
 198 probability, to continuously stay inside the
 199 communication circle before finally moving out of it.
 200 Furthermore, its complementary cumulative distribution
 201 function (CCDF) is denoted by $F_L(t)$

$$F_L(t) = P(T_L \geq t) \tag{2}$$

203 The link outage probability P_{L_p} associated with a
 204 particular packet length L_p can be evaluated as

$$P_{L_p} = P\left(T_L < \frac{L_p}{B}\right) = 1 - F_L\left(\frac{L_p}{B}\right) \tag{3}$$

206
 207 **3.1 Distribution of relative velocity**

208 Figure 1 shows the transmission zone of a node (node m_a)
 209 which is a circle of radius R centered at the node. The
 210 figure shows another node (say node m_b) starting to com-
 211 municate data with node m_a at time t_2 . As shown in the left
 212 side of the figure, at time t_2 , node m_a is moving at speed v_a

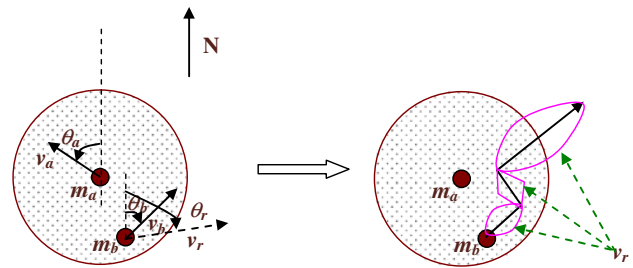


Fig. 1 Graphical illustration of relative velocity

with direction θ_a , while node m_b moves at speed v_b with
 direction θ_b .

Alternatively, if we consider node m_a as static, node m_b
 is moving at their *relative speed* and *direction* v_r and θ_c ,
 respectively. An example of resulting trajectories of node
 m_b moving at relative velocity is given in the right side of
 Fig. 1. With the assumption that both θ_a and θ_b are uni-
 formly distributed within $[0, 2\pi)$, it can be concluded that
 the composite direction $\theta_c = \theta_b - \theta_a$ is also uniformly
 distributed within $[0, 2\pi)$. In this case, the relative speed v_r
 can be expressed as

$$v_r = \sqrt{v_a^2 + v_b^2 - 2v_a v_b \cos \theta_c} \tag{4}$$

Conditioning on v_a and v_b and noting the symmetric
 property of θ_c , the distribution of v_r can be computed as

$$p(v_r) = E_{\{v_a, v_b\}}(p(v_r | v_a, v_b)) \tag{5}$$

$$p(v_r | v_a, v_b) = p(\theta_c) \left| \frac{d\theta_c}{dv_r} \right|$$

$$= \frac{1}{\pi} \left| \frac{d}{dv_r} \left(\arccos \left(\frac{v_a^2 + v_b^2 - v_r^2}{2v_a v_b} \right) \right) \right|$$

$$= \begin{cases} g(v_r, v_a, v_b), & |v_a - v_b| \leq v_r \leq v_a + v_b \\ 0, & \text{otherwise} \end{cases} \tag{6}$$

where $g(x, y, z) = \frac{2}{\pi} \frac{x}{\sqrt{2(x^2 y^2 + x^2 z^2 + y^2 z^2) - x^4 - y^4 - z^4}}$. 230

In particular, if both nodes move at the same speed
 $v = v_a = v_b$, we will have

$$p(v_r | v) = \begin{cases} \frac{2}{\pi} \frac{1}{\sqrt{4v^2 - v_r^2}}, & v_r \in [0, 2v] \\ 0, & \text{otherwise} \end{cases} \tag{7}$$

3.2 Distribution of link lifetime (LLT)

The essence of modeling link dynamics in MANETs con-
 sists of evaluating the distribution of LLT, because it
 reflects the link dynamics resulting from the motions of
 nodes. LLT measures the duration of time for a node to
 continuously stay inside the communication range of
 another node. In our model, this range is a circle.

Author Proof

¹ In mobile ad hoc network, the traffic is generated randomly and nodes are moving randomly. When a node initiate traffic to other nodes, the target node could be anywhere in the network and the relays could also be anywhere in the communication range. Therefore, a uniform distribution assumption naturally fits into the scenario.

Clearly, different mobility models and parameters lead to different LLT distributions, and the main challenge in modeling LLT consists of making the problem tractable and relevant. We know that the relative movement of nodes consists of a sequence of mobility trips, derived from the chain of mobility trips of the two communicating nodes. Let A_s be the starting point of the current mobility trip and the end point of the current trip be denoted by A_d . We have that A_d may be anywhere in the cell, i.e., inside or out of the communication circle. In the case that A_d is located inside the communication circle, it serves as the starting point (i.e., a new A_s) for the next trip and the whole process is repeated. In the evaluation of LLT, this process is repeated until the final A_d is outside of the communication circle.

As illustrated in Fig. 2, the procedure for evaluating the LLT can be modeled as a two-state Markovian process. The residence state \mathbf{S}_0 represents the scenario where the end point A_d of the current trip is located inside the communication circle, while the departing state \mathbf{S}_1 refers to the complementary scenario in which A_d is outside of communication circle. Compared to the model by Samar and Wicker [5, 6], in which only the last scenario (i.e., state \mathbf{S}_1) is considered, the two-state Markovian model reflects the motion of nodes more accurately, which leads to better results in evaluating link dynamics.

Let P_s be the residence probability, which denotes the probability that A_d is located inside the communication circle. The probability distribution function (PDF) $S_0(t)$ specifies the distribution of sojourn time of mobility epochs when a node stays in state \mathbf{S}_0 . Correspondingly, the PDF $S_1(t)$ is used to measure the distribution of the departing time, when node moves out of communication circle and switches to state \mathbf{S}_1 .

Before eventually moving out of the communication circle (i.e., being switched to the departing state \mathbf{S}_1), nodes may stay at the residence state \mathbf{S}_0 multiple times. Let N_i be the integer variable counting the number of times for a node to remain in state \mathbf{S}_0 , and let $\{s_{0,0}, \dots, s_{0,N_i-1}\}$ be the associated random variables that specify the duration of time of trips for each return.

Clearly, $\{s_{0,0}, \dots, s_{0,N_i-1}\}$ are random variables of the same distribution but correlated. However, to make our problem more tractable, we assume that $\{s_{0,0}, \dots, s_{0,N_i-1}\}$ are statistically i.i.d random variables of distribution $S_0(t)$.

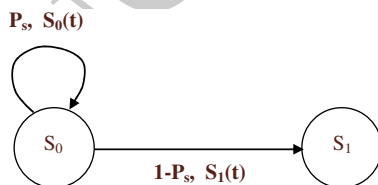


Fig. 2 Two-state Markovian model for LLT evaluation

Our simplifying assumption makes the final result slightly deviated from the real situation when the residence probability becomes larger. However, as we will see later, our model still provides a good approximation, even with a large residence probability.

We define s_1 as the random variable measuring the departing time of distribution $S_1(t)$. The conditional link life time $T_L(N_i)$ and $P(N_i = K)$ can be evaluated as follows:

$$T_L(N_i) = \sum_{i=0}^{N_i-1} s_{0,i} + s_1, \tag{8}$$

$$P(N_i = K) = P_s^K. \tag{9}$$

The characteristic function $U_{T_L}(\theta)$ for the LLT T_L can then be evaluated as

$$\begin{aligned} U_{T_L}(\theta) &= E(e^{j\theta T_L}) \\ &= \sum_{k=0}^{\infty} E(e^{j\theta(\sum_{i=0}^{k-1} s_{0,i} + s_1)}) P(N_i = k) \\ &= \sum_{k=0}^{\infty} U_1(\theta) U_0(\theta)^k P_s^k \\ &= \frac{U_1(\theta)}{1 - U_0(\theta) P_s}, \end{aligned} \tag{10}$$

where $U_0(\theta)$ and $U_1(\theta)$ are the characteristic functions of $S_0(t)$ and $S_1(t)$, respectively.

When the communication circle is small with respect to the network size and nodes' speed, A_d is mostly located outside of the communication circle. Consequently, we have $P_s \ll 1$. Given that $U_0(\theta)$ is the characteristic function of $S_0(t)$, it follows that $|U_0(\theta)| \leq 1$. Finally, it is clear that $U_0(\theta) P_s \ll 1$. Therefore, Eq. 10 can be approximated as

$$U_{T_L}(\theta) \approx U_1(\theta) \tag{11}$$

For clarity, we call Eq. 10 Exact LLT (ES-LLT), which is based on the two-state Markovian model. The approximation in Eq. 11 is called Approximated LLT (AS-LLT), and it reflects the scenario considered by Samar and Wicker [5, 6]. As we will see later, for the random direction mobility model (RDMM), the analytical expression of AS-LLT is the same as the expression in [5, 6], except for a normalization factor.

3.3 Practical implications

It is clear that the two-phase Markov model is a general model that can be applied to networks with different mobility models by adapting its two building blocks $S_0(t)$ and $S_1(t)$ to the specific network and mobility models, including but not restricted to the random trip mobility model.

326 However, in some practical scenarios, the analytical
 327 formulations of $S_0(t)$ and $S_1(t)$ might not be available.
 328 Under such circumstances, one can collect a trace data to
 329 obtain $S_0(t)$ and $S_1(t)$ and still give an accurate estimate of
 330 the overall link lifetime. By doing so, it can greatly reduce
 331 the amount of empirical data necessary to accurately esti-
 332 mate link lifetime. Furthermore, one can also obtain
 333 analytical formulations by curve-fitting empirical data and
 334 incorporate these formulations to our Markov model for an
 335 analytical study of the mobility characteristics.

336 3.4 Link lifetime in random direction mobility model

337 The random direction mobility model (RDMM) is an
 338 important mobility model for MANETs. It improves ran-
 339 dom waypoint mobility (RWP) model on the stationary
 340 uniform nodal distribution, and has been widely adopted
 341 [12–16]. However, the analysis on the characteristic of link
 342 lifetime of RDMM is quite limited. In this section, we
 343 provide a deeper understanding of RDMM by providing an
 344 analytical expression for characterizing its link lifetime.

345 In RDMM, node movements are independently and
 346 identically distributed (iid) and can be described by a
 347 continuous-time stochastic process. The continuous
 348 movement of nodes is divided into mobility epochs during
 349 which a node moves at constant velocity, i.e., fixed speed
 350 and direction. But the speed and direction varies from
 351 epoch to epoch. The time duration of epochs is denoted by
 352 a random variable τ , assumed to be exponentially distrib-
 353 uted with parameter λ_m . Its CCDF $F_m(\tau)$ can be written as
 354 [14]

$$F_m(\tau) = \exp(-\lambda_m \tau). \tag{12}$$

355 The direction during each epoch is assumed to be
 356 uniformly distributed over $[0, 2\pi)$ and the speed of each
 357 epoch is uniformly distributed over $[v_{\min}, v_{\max}]$, where v_{\min}
 358 and v_{\max} denote the minimum and the maximum speed of
 359 nodes, respectively. Speed, direction and epoch time are
 360 mutually uncorrelated and independent over epochs, and
 361 the location and direction of nodes is uniformly distributed
 362 [17].

364 To evaluate the LLT T_L , we need to evaluate P_s , $S_0(t)$, and
 365 $S_1(t)$. Let z_d denote the least distance to be traveled by node
 366 to move out of the communication circle, starting from the
 367 position A_s and without changing the direction and speed v_r .
 368 A graphical illustration of z_d is presented in Fig. 3. The
 369 probability P_s can now be evaluated through z_d as

$$P_s = E_{z_d}(P_s(z_d)) = \int_{z_d} P_s(z_d) p(z_d) dz_d \tag{13}$$

371

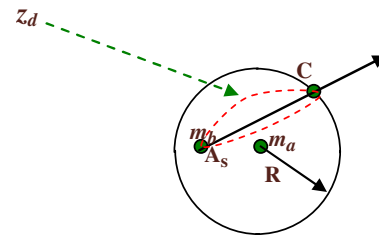


Fig. 3 Graphical illustration of z_d

$$\begin{aligned} P_s(z_d) &= \int_{v_r} P\left(\tau \leq \frac{z_d}{v_r}\right) p(v_r) dv_r \\ &= \int_{v_r} \left(1 - F_m\left(\frac{z_d}{v_r}\right)\right) p(v_r) dv_r \\ &= \int_{v_r} (1 - \exp(-2\lambda_m z_d / v_r)) p(v_r) dv_r, \end{aligned} \tag{14}$$

where $P_s(z_d)$ is the conditional probability of P_s on z_d , and $p(z_d)$ is the PDF of z_d . The evaluation of z_d directly follows from [18]:

$$p(z_d) = \begin{cases} \frac{2}{\pi R^2} \sqrt{R^2 - \left(\frac{z_d}{2}\right)^2}, & \text{for } 0 \leq z_d \leq 2R \\ 0, & \text{elsewhere} \end{cases} \tag{15}$$

$S_0(t)$ is the PDF of the time duration for nodes to return to state S_0 . Conditioning on z_d and assuming that the starting time is at time 0, $S(t)$ is the probability of node m_b changing its relative velocity at time t on condition that A_d is located inside the communication circle. Therefore,

$$S_0(t) = E_{z_d}(S_0(t|z_d)) \tag{16}$$

$$\begin{aligned} S_0(t|z_d) &= \frac{1}{P_s} P(t = \tau, z_d \geq v_r \tau | z_d) \\ &= \frac{1}{P_s} P(\tau = t) P\left(v_r \leq \frac{z_d}{t} | z_d\right) \\ &= \frac{1}{P_s} 2\lambda_m e^{-2\lambda_m t} \int_0^{\min\{V_m, \frac{z_d}{t}\}} p(v_r) dv_r, \end{aligned} \tag{17}$$

where $S_0(t|z_d)$ is the conditional PDF on z_d and V_m is the maximum speed of v_r .

$S_1(t)$ can be evaluated in much the same way as we have done for $S_0(t)$. Conditioning on z_d and assuming that the starting time is at time 0, $S_1(t)$ is simply the probability of the node m_b moving out of the communication circle at time t with relative velocity being kept constant. Similar to the previous case, we have

$$S_1(t) = E_{z_d}(S_1(t|z_d)) \tag{18}$$

377

378

379

380

381

382

383

384

385

386

387

388

389

390

391

392

393

394

395

396

397

398

399

400

$$\begin{aligned}
 S_1(t|z_d) &= \frac{1}{1 - P_s} P\left(t = \frac{z_d}{v_r}, z_d \leq v_r \tau | z_d\right) \\
 &= \frac{1}{1 - P_s} P(\tau \geq t) p\left(v_r = \frac{z_d}{t}\right) \left| \frac{d}{dt} \left(\frac{z_d}{t}\right) \right| \quad (19) \\
 &= \frac{1}{1 - P_s} \exp(-2\lambda_m t) p_{v_r}\left(\frac{z_d}{t}\right) \frac{z_d}{t^2},
 \end{aligned}$$

397 where $S_1(t|z_d)$ is the conditional PDF on z_d using the
 398 Jacobian of the transformation.

399 Let us define v_{s_1} to be the conditional relative velocity
 400 associated with state \mathbf{S}_1 such that $p(v_{s_1}) = p(v_r | S_1)$ and it
 401 should be noted that the distribution of v_{s_1} can be greatly
 402 different from the distribution of $p(v_r)$. Accordingly, an
 403 alternative way to evaluate $S_1(t)$ is:

$$S_1(t) = E_{v_{s_1}}(S_1(t|v_{s_1})) \quad (20)$$

$$\begin{aligned}
 S_1(t|v_{s_1}) &= \frac{1}{1 - P_s} P\left(t = \frac{z_d}{v_{s_1}} \mid z_d \leq v_{s_1} \tau\right) \\
 &= \frac{1}{1 - P_s} P(\tau \geq t) p(z_d = v_{s_1} t) \frac{d}{dt}(v_{s_1} t) \\
 &= \begin{cases} \frac{4e^{-2\lambda_m t} v_{s_1}}{\pi(1 - P_s) 2R} \sqrt{1 - \left(\frac{v_{s_1} t}{2R}\right)^2}, & 0 \leq t \leq \frac{2R}{v_{s_1}} \\ 0, & \text{elsewhere} \end{cases}
 \end{aligned}$$

407 where $S_1(t|v_{s_1})$ is the conditional PDF of $S_1(t)$ on v_{s_1} .
 408 A detailed examination of Eq. 20 reveals that it shares the
 409 same core analytical expression of link lifetime distribution
 410 of Eq. 15 in [6], with the only exception that a normaliza-
 411 tion factor $e^{-2\lambda_m t} / (1 - P_s)$ accounts for the probability
 412 of nodes leaving for state \mathbf{S}_1 . It implies that AS-LLT for-
 413 mula, solely relying on $S_1(t)$, gives the same link lifetime
 414 distribution as in [6].

415 4 Path lifetime in MANETs

416 We have examined the dynamics of link lifetime for a
 417 point-to-point link. However, for most cases in MANETs, a
 418 packet needs to be forwarded by several intermediate nodes
 419 before finally reaching the destination. The source node,
 420 intermediate nodes and destination node collectively form
 421 a multi-hop path for the packet. Clearly, path dynamics is
 422 also an essential metric for protocol design and optimiza-
 423 tion. Han et al. showed [19, 20] that path dynamics
 424 converge asymptotically to an exponential distribution,
 425 when links are assumed to be independent or of limited
 426 dependence. The result works well when a path involves a
 427 significant number of hops but not for paths with a small to
 428 moderate number of hops. In this section, we will extend
 429 the proposed analytical framework to evaluate path
 430 dynamics with small to moderate numbers of hops,
 431 assuming that each link along the path behaves independ-
 432 ently of others. In reality, adjacent links have some

433 correlation, which is difficult to model. Modeling depen-
 434 dent links requires a number of conditional probability
 435 distributions, and a solution may not be feasible. The
 436 independence assumption that we make greatly simplifies
 437 the analysis and still provides a good approximation.

438 As illustrated in Fig. 4, a packet from source node M_1 needs
 439 to follow the ordered set of links $\{T_1 \rightarrow T_2 \rightarrow \dots \rightarrow T_{K-1}\}$
 440 to reach the destination node M_K . Successful delivery of the
 441 packet requires that none of these links on the path breaks
 442 during packet transmission. When any of the links breaks, the
 443 path no longer exists and the path discovery process needs to be
 444 reinitiated to find alternative paths. In other words, lifetime
 445 $T_P(K)$ of the $(K - 1)$ -hop path is the minimum lifetime of the
 446 links that form it, and can be written as

$$T_P(K) = \min\{T_1, \dots, T_{K-1}\} \quad (21)$$

448 Because links are assumed to operate independently with
 449 i.i.d motion, their lifetime also follows the same statistical
 450 distribution as T_L . However, when the source node initiates
 451 a data transfer to the destination node, links may have been
 452 in existence for some time; therefore, as Fig. 4 illustrates,
 453 the lifetime $T_i, i \in \{1, \dots, K - 1\}$ of the directional link on
 454 the data path should be the *residual lifetime* of the link, i.e.,
 $T_i = T_L(\epsilon_i), i \in \{1, \dots, K - 1\}$ (22)

456 where $\epsilon_i \geq 0$ is a random variable representing the elapsed
 457 time of the link $M_i \rightarrow M_{i+1}$ before the data path started and
 458 clearly, $T_L = T_L(0)$.

459 From Sect. 3, we know that the evaluation of $T_L(\epsilon_i)$
 460 depends on a set of three parameters, i.e., the spatial dis-
 461 tribution of nodes at time ϵ_i , the distribution of speed $v_r(\epsilon_i)$
 462 at time ϵ_i , and the residual change time distribution $\tau(\epsilon_i)$ at
 463 ϵ_i . At time 0 and ϵ_i , nodes are expected to follow the same
 464 stationary distribution and therefore resemble each other.
 465 Similarly, it can be expected that the speed distribution of

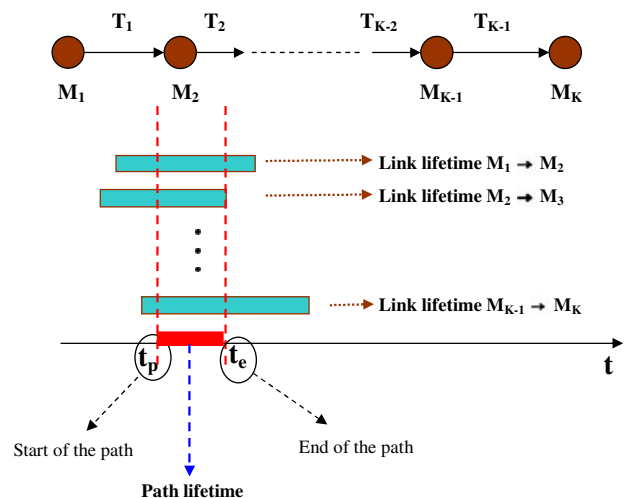


Fig. 4 Path structure

466 v_r will be also the same. Therefore, we expect that the
 467 distribution of $\tau(\varepsilon_i)$ and $\tau(0)$ will resemble each other. In
 468 particular, we know that the distribution of $\tau(0)$ for the
 469 RDMM model is exponentially distributed. Accordingly,
 470 because of the memoryless property of the exponential
 471 distribution, the distribution of $\tau(\varepsilon_i)$ and $\tau(0)$ will exactly
 472 resemble each other. Finally, we conclude that the distri-
 473 bution of T_i will resemble the distribution of $T_L = T_L(0)$.

474 Summarizing the above discussion, the CCDF $F_P(K, t)$ of
 475 the lifetime for a $(K - 1)$ -hop path can be computed as

$$F_P(K, t) = F_L^{K-1}(t). \tag{23}$$

477 **5 Model validation**
 478

479 **5.1 Simulation setup**

480 In the simulation, there are 100 nodes randomly placed in a
 481 $1,000 \times 1,000$ m square cell. Each node has the same
 482 transmit power and two profiles of radio transmission range
 483 are chosen for the simulation experiments. Both are within
 484 the coverage of IEEE 802.11 PHY layer and they are
 485 $\{200 \text{ m}, 100 \text{ m}\}$. After initial placement, nodes keep mov-
 486 ing continuously according to the RDMM model. The
 487 mobility parameter λ_m is the same as the one in [21]
 488 ($\lambda_m = 4$), which means that nodes change their velocity at
 489 every $\frac{1}{4}$ h in average. Furthermore, we assume that every
 490 node is moving at the same constant speed and only its
 491 direction is changed according to the RDMM model. The
 492 simulation with variable speeds can be obtained by averaging
 493 the results from every speed with respect to the distribution of
 494 speed v . However, it should be noted that the relative speeds
 495 between nodes are not constant and their statistics are derived
 496 in Sect. 3.1. Three different speeds are simulated $v \in \{1, 10,$
 497 $20\}$ (m/s), which range from pedestrian speed to vehicle
 498 speed. Combining the power profile and velocity profile, six
 499 different scenarios are simulated $\{I: (200 \text{ m}, 1 \text{ m/s}); II:$
 500 $(100 \text{ m}, 1 \text{ m/s}); III: (200 \text{ m}, 10 \text{ m/s}); IV: (100 \text{ m}, 10 \text{ m/s}); V:$
 501 $(200 \text{ m}, 20 \text{ m/s}); VI: (100 \text{ m}, 20 \text{ m/s})\}$.

502 Nodes are randomly activated for data transmission. The
 503 traffic of activated nodes is supplied from a constant bit
 504 rate (CBR) source with a packet rate of 0.5 p/s. Given that
 505 the choice of specific MAC layer and routing protocol may
 506 affect the results, we assume perfect MAC and routing
 507 protocols, rendering zero delays or losses due to their
 508 functionalities. This enables the simulation to capture statis-
 509 tics solely due to mobility.

510 **5.2 Accuracy of models**

511 Table 1 describes the residence probability P_s for all six
 512 scenarios. As shown in Eqs. 16 and 18, the characteristics

Table 1 Residence Probability P_s

Radius R (m)	Speed v (m/s)		
	$v = 1$	$v = 10$	$v = 20$
$R = 100$	$P_s = 0.194$	0.033	0.018
$R = 200$	$P_s = 0.3072$	0.058	0.033

of mobility are governed by the ratio between the radius R
 of the communication circle and the speed v , which we call
 the relative radius (ReR) $\frac{R}{v}$. Among the six different scenar-
 ios, there are five different ReR values $\{5, 10, 20, 100, 200\}$,
 given that IV and V scenario have the same ReR and exhibit
 similar results, as will be seen from simulations. As shown in
 Table 1, the residence probability increases with ReR, indicat-
 ing that it is more likely for nodes with larger ReR to stay
 inside the communication circle.

Figure 5 presents the results for link lifetime ES-LLT and
 AS-LLT predicted by our analytical model, as well as by the
 simulations. The results clearly confirm that the two-state
 Markovian model is a powerful tool to model link dynamics of
 the link lifetime distribution as a function of node mobility.
 It can be also observed that the ES-LLT formula, obtained
 from the Markovian model, shows a very good match with
 simulations in all scenarios. On the other hand, the AS-LLT
 formula, which corresponds to the model by Samar and Wicker
 [5, 6] gives good approximations to the simulations only for
 small values of ReR ($\frac{R}{v}$), and greatly deviates from the
 simulations when ReR becomes large, i.e., larger residence
 probability P_s and larger possibility for nodes to stay inside
 communication circle.

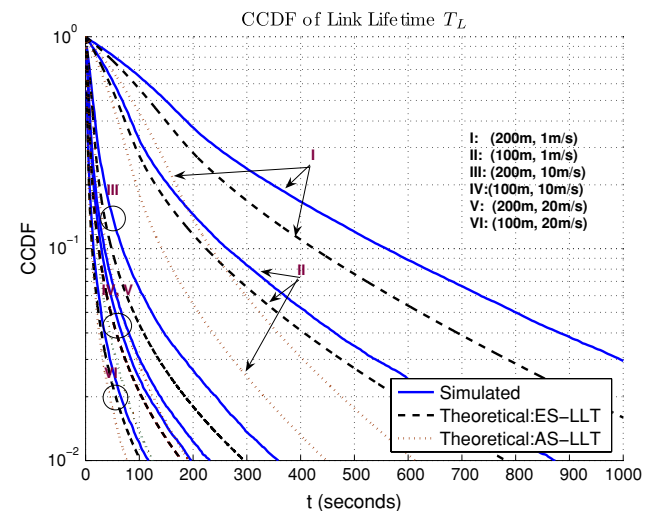


Fig. 5 Link lifetime T_L (RDMM): simulated, ES-LLT(Markovian), and AS-LLT

Author Proof

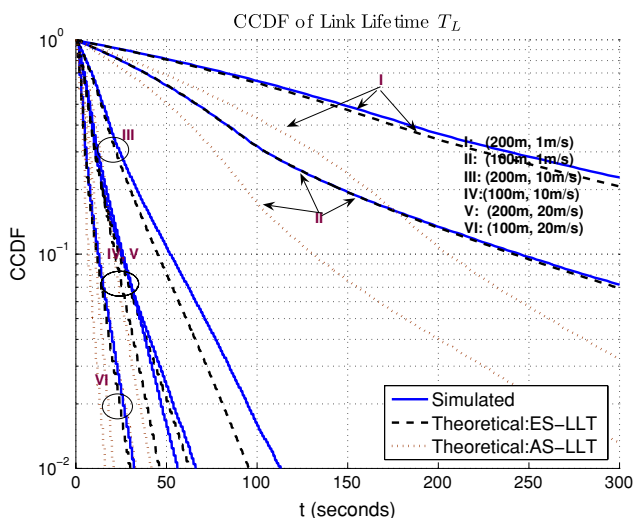


Fig. 6 Link lifetime T_L (RWP): simulated, ES-LLT(Markovian), and AS-LLT

538 As stated in Sect. 3.3, in some practical scenarios, the
 539 analytical formulations of $S_0(t)$ and $S_1(t)$ might need to be
 540 obtained from empirical data to characterize the overall
 541 link lifetime. Figure 6 presents such a result, where trace
 542 data are generated from the random waypoint (RWP)
 543 model. Because there is no analytical formulations of $S_0(t)$
 544 and $S_1(t)$ for RWP, the two-phase Markov model is applied
 545 by using empirical simulated data to estimate the link
 546 lifetime. The results clearly confirm the accuracy, effective-
 547 ness and generality of our Markov model to analyze
 548 more practical mobility models.

549 Figures 7 and 8 present the results of path lifetime. It
 550 can be observed that path lifetime can be modeled accu-
 551 rately with the proposed Markovian model, and is only

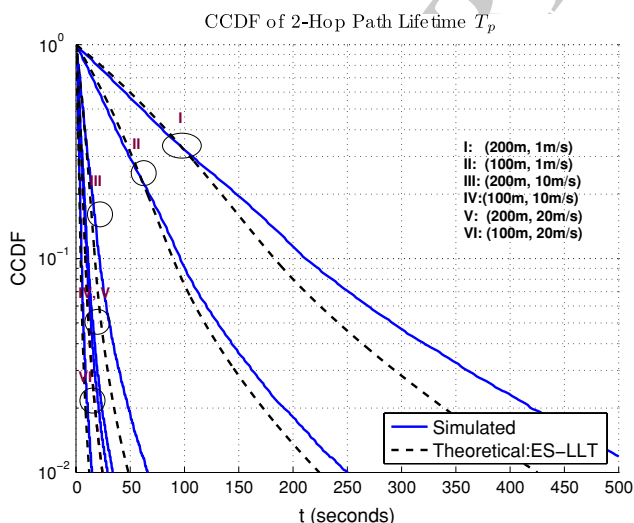


Fig. 7 Simulation: 2-hop path lifetime

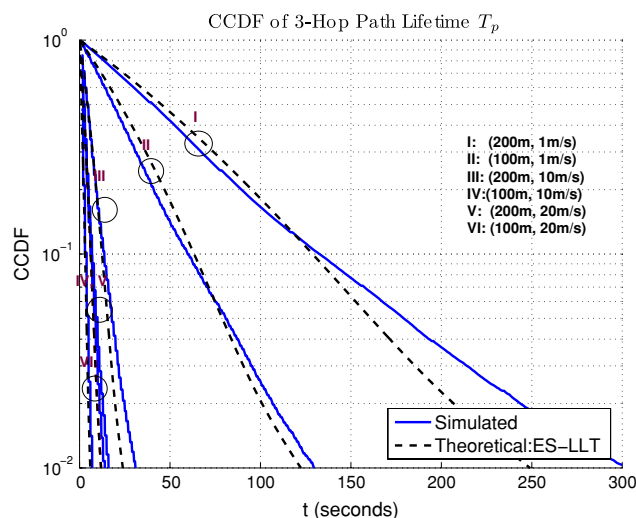


Fig. 8 Simulation: 3-hop path lifetime

slightly affected by the independence assumption used to 552
 derive it. 553

In summary, the Markovian model (ES-LLT formula) is 554
 more accurate model than the AS-LLT formula [5, 6] for 555
 all ranges of ReR and shows good approximations to all 556
 simulations, in contrast to the AS-LLT formula that gives 557
 good approximation only when ReR is relatively small. 558

6 Packet-length optimization 559

6.1 Link lifetime and packet length 560

Given that nodes move in a MANET, the data transfer can 561
 be temporarily broken if any link on the path to the des- 562
 tination is broken. An alternative path may not be available 563
 immediately, and significant delay can be incurred in 564
 repairing a route. Within the context of MANETs, it is 565
 important to use information packet lengths that maximize 566
 the end-to-end throughput. If a information data-packet 567
 length is too long, frequent link breaks can lead to signif- 568
 icant packet dropout during the transfer. On the other hand, 569
 if data packet length is too short, the packet-header over- 570
 head and channel access overhead can reduce the effective 571
 throughput significantly. Hence, a judicious choice of 572
 information packet length as a function of link dynamics 573
 can be of great importance in maximizing throughput in 574
 MANETs. However, this problem has been overlooked in 575
 the past, because its solution requires knowledge of statis- 576
 tics of link lifetime. With the computed CCDF in Sect. 3, 577
 we are able to provide packetizing schemes optimized on 578
 various systematic constraints. 579

When the length of packets is constant, it is natural to 580
 ask what the optimal packet length would be. For every 581
 packet length L_p , we know that there is an associated link 582

583 outage probability P_{L_p} specifying the probability of link
 584 breach during packet transfer. Every dropped packet during
 585 link outage is either lost or must be retransmitted and
 586 therefore reduces the effective throughput. The optimal
 587 packet length is chosen such that the total throughput is
 588 maximized.

589 One approach is to simply choose the maximum possible
 590 packet length L_0 that satisfies a pre-defined link
 591 outage probability requirement. We call this strategy link
 592 outage priority design (LOPD) and it can be described as

$$L_0 = \max_{L_p} P_{L_p} \leq \omega_p \quad (24)$$

594 where ω_p is a constant specifying the link dropout proba-
 595 bility requirement.

596 Alternatively, we can use a cost function $C(L_p, P_{L_p})$ that
 597 incorporates the negative effect from the packet retrans-
 598 mission into evaluating the effective throughput $ET(L_p)$ for
 599 a specific packet length L_p . The cost function $C(L_p, P_{L_p})$
 600 could be a systematic constraint from upper layer, such as
 601 the negative effects from delay and packet retransmissions.
 602 Further optimizing the effective throughput $ET(L_p)$ gives
 603 the optimal packet length L_0 . Consequently, we refer to this
 604 strategy link throughput priority design (LTPD).

605 In LTPD, when the packet length is L_p , we can describe
 606 the effective throughput $ET(L_p)$ function as

$$ET(L_p) = (1 - P_{L_p}) \cdot L_p - C(L_p, P_{L_p}) \cdot P_{L_p} \cdot L_p \quad (25)$$

608 The optimal packet length L_0 will be the one that
 609 maximizes the effective throughput

$$L_0 = \max_{L_p} ET(L_p) \quad (26)$$

611 Normally, P_{L_p} is a monotonically decreasing function
 612 w.r.t. packet length. When the cost function is chosen to be
 613 a constant penalty value, i.e., $(C(L_p, P_{L_p}) = C)$ by taking

the derivative with respect to L_p , the optimal packet length
 L_0 is the value satisfying

$$1 - (1 + C)P_{L_0} = (1 + C)L_0 \frac{dP_{L_p}}{dL_p} \Big|_{L_p=L_0} \quad (27)$$

In Fig. 9, we exploit the application of the link lifetime
 distribution to the optimization of packet-length design
 using the same examples of the previous section. For
 illustration purposes, the cost function for our example of
 LTPD is chosen as a constant penalty value of 2 (i.e.,
 $C(L_p, P_{L_p}) = 2$). However, it should be noted that the
 practical cost function can be much more complicated and
 determined by upper layers for a cross-layer optimization
 solution. However, computing the optimum choice for
 $C(L_p, P_{L_p})$ is beyond the scope of this paper. The effective
 throughput $ET(L_p)$ is computed for every L_p and drawn for
 all three methods: Simulated, ES-LLT (Markovian model)
 and AS-LLT. As expected, ES-LLT approximates the
 simulation very well, while AS-LLT tends to
 conservatively underestimate the effective throughput for
 larger ReR. In addition, all curves of the effective
 throughput (either Simulated, ES-LLT or AS-LLT
 formula) are convex functions with numerical solutions
 readily available.

The optimized solutions $\frac{L_0}{B}$ on packet design for all
 design methods are illustrated in Fig. 10. In the simulation,
 the link outage tolerance of LOPD is set to be $\omega_p = 0.1$,
 i.e., the maximum link outage probability should be less
 than 10%. Two key observations should be made: First, the
 ES-LLT (Markovian model) approaches the simulated
 optimal solution well for LTPD and LOPD, and signifies
 substantial improvement of throughput over the AS-LLT
 model [5, 6]. Second, LTPD suggests a balanced design
 between longer packet and larger retransmission rate to
 offer higher throughput over LOPD. On the other hand,
 LOPD tends to be more conservative on throughput but
 renders fewer packet retransmissions.

Another important observation from Fig. 10 is that the
 optimal solutions, obtained from either the simulation or
 Markovian ES-LLT formula, exhibit linear proportion to
 the ReR value $\frac{R}{v}$. It suggests that mathematically, the
 optimal packet design should follow the rule²

$$\frac{L_0}{B} = \Theta \left(\frac{R}{v} \right) \quad (28)$$

6.2 Path lifetime and packet length

We can also investigate the optimal packet length for a
 given path and the effect of hop count on the optimal

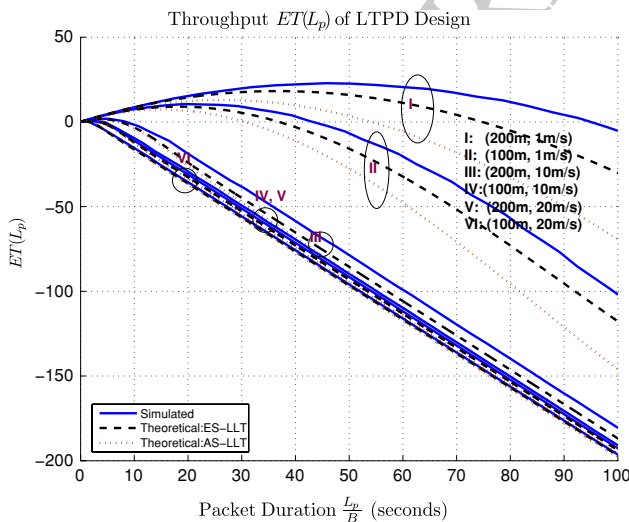


Fig. 9 LTPD design

² We recall that $f(n) = \Theta(g(n))$ means there exist positive constants c_1, c_2 and M , such that $0 \leq c_1 g(n) \leq f(n) \leq c_2 g(n) \forall n > M$.

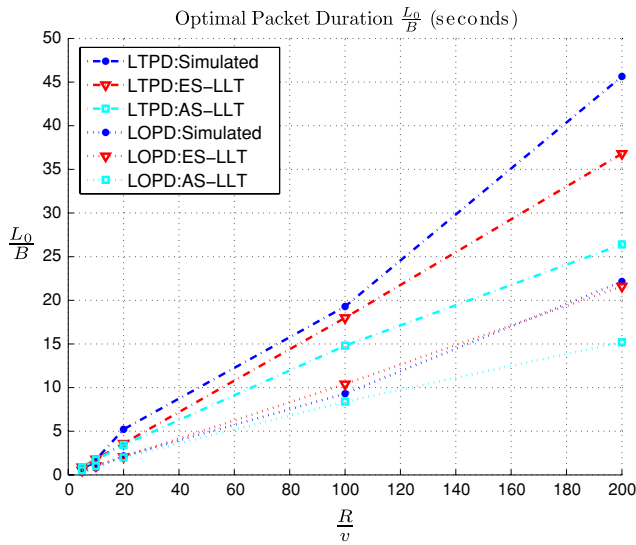


Fig. 10 Optimal packet duration $\frac{L_0}{B}$

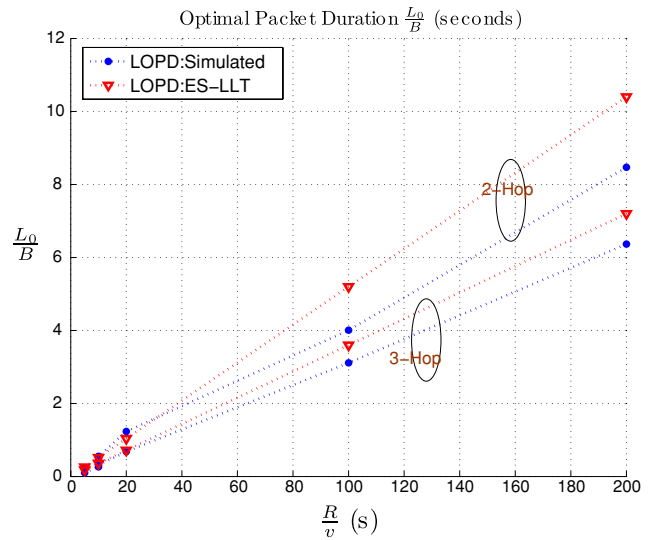


Fig. 11 Optimal packet length for multi-hop paths

659 packet length. Extending the optimal packet design
 660 example in Sect. 6 for a 2-hop path, the results we obtain
 661 are shown below.

662 In Fig. 11, we only present the results following LOPD,
 663 because the penalty of a path breakage is usually pretty
 664 high and a more practical design is to ensure that packet
 665 can get through the path with low outage probability. For
 666 example, in AODV [22], the source needs to flood the
 667 network to reinitiate a route to the destination, when an
 668 existing path breaks. Furthermore, similar to the case of
 669 link lifetime, the linear relationship between the optimal
 670 packet length and network parameters can also be
 671 observed. Although only the results for 2-hop and 3-hop
 672 paths are shown here, we have examined cases with dif-
 673 ferent hop counts (various K) and they all exhibit similar
 674 behavior.

675 Another aspect examined here is the effect of hop count
 676 on the choice of optimal packet length. In Fig. 12, for each
 677 K -hop path, the optimal packet length is chosen based on
 678 LOPD design criterion. We can see that the packet length
 679 should also be chosen such that³
 680

$$\frac{L_0 K}{B} = \Theta(1). \quad (29)$$

682 Combining our observations from Figs. 11 and 12, we
 683 conclude that the packet length for a K -hop path should be
 684 designed as
 685

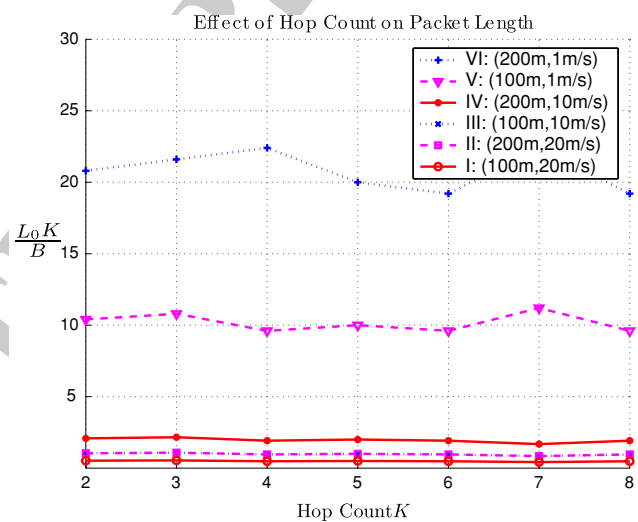


Fig. 12 Effect of hop count on packet length

$$\frac{L_0}{B} = \Theta\left(\frac{R}{vK}\right). \quad (30)$$

7 Cache lifetime optimization

687 From the previous analysis, we observe that the optimal
 688 packet length should be chosen based on the knowledge of
 689 hop distance between source and destination. Similarly, the
 690 route caching scheme of on-demand routing protocols
 691 should follow the same rule. However, without knowing the
 692 relationship represented in Eq. 30, it is difficult to determine
 693 the timeout value for different routes. As a result,
 694 on-demand protocols like DSR [23] use the same value for
 695 the parameter *RouteCacheTimeout* to set the timeout for all
 696 cached routes. However, based in Eq. 30, we know that the
 697
 698

3FL01 ³ Equivalently, we can transfer K to the other side of this equation. It
 3FL02 means that when the number of hops increases for a constant
 3FL03 bandwidth B , the packet length should decrease.

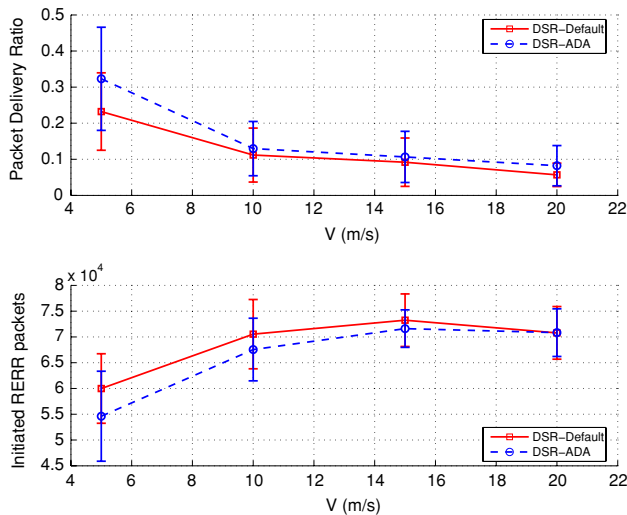


Fig. 13 Illustrative example of cache guideline

699 cache timeout scheme for DSR and any on-demand routing
 700 protocol should be adapted to the hop count of the cached
 701 routes. An example of a mobility-adaptive cache timeout
 702 scheme for DSR derived based on the analytical guidance
 703 that we gain from our model is the following:

- 704 • A base parameter *RouteCacheTimeout* takes user input
 705 to set timeout value for a point to point link (one-hop
 706 path). Such value can be either chosen in ad hoc
 707 manner or determined from LTPD or LOPD design of
 708 Sect. 6.
- 709 • The timeout value T_k of a route is determined based on the
 710 base parameter and the number (K) of links involved on
 711 the route. And it can be expressed as $T_k = \text{RouteCache-}$
 712 $\text{Timeout}/K$.

713 Figure 13 presents results of this illustrative hop-adaptive
 714 caching strategy for DSR. In the simulation, 50 nodes are
 715 randomly moving in a 1500×500 m area according to the
 716 random waypoint model without pause. The minimum speed
 717 is zero and the maximum speed V varies. The source and
 718 destination pairs are randomly chosen. Ten pairs are simulated
 719 and traffics are supplied from CBR source at a rate 4 p/s. Each
 720 packet is of size 64 bytes and all simulations run for 900 s. Ten
 721 random seeds are simulated for each configuration. The
 722 implementation of DSR used for comparison is the default
 723 implementation in *Qualnet 3.9.5*.

724 Figure 13 compares the default DSR (DSR-Default) and
 725 the hop-adaptive DSR (DSR-ADA). It can be observed that,
 726 by effectively timing out stale paths, DSR-ADA reduces the
 727 overhead incurred from route error (RERR) packets and
 728 improves the overall packet delivery ratio. This further con-
 729 firms that our modeling framework can be used to improve
 730 existing routing protocols. However, it should be noted that
 731 the above DSR-ADA cache strategy is by no means a perfect
 732 solution to the caching problem in on-demand routing. It is

733 meant simply as an example to illustrate the effectiveness of
 734 analytical results that are derived in this paper.

8 Analysis of throughput, average delay, and storage 735

736 We consider the well-known two-hop forwarding scheme
 737 introduced by Grossglauser and Tse [8, 9] in the computa-
 738 tion of the throughput of a MANET. Following a bottom-up
 739 approach and utilizing our analytical results on the optimal
 740 packet length in Sect. 6, we rediscover exactly the same
 741 result on the throughput, showing the effectiveness of our
 742 models on the computation of throughput and capability to
 743 handling more complex schemes. Furthermore, we give a
 744 comprehensive packet-level and bit-level analysis on the
 745 delay and storage requirement, in contrast to most studies
 746 where only the packet level analysis can be conducted.

8.1 Throughput 747

748 Because the two-hop forwarding scheme is such that
 749 packets are transferred only when nodes are close to each
 750 other, the packet length L_0 should be chosen according to
 751 the results from the analysis of link lifetime, i.e.,
 752 $L_0 = \Theta\left(\frac{R \cdot B}{E(v)}\right)$. Based on the mobility models in [21], we
 753 have one data packet transferred on average for every time
 754 duration of $I = \Theta\left(\frac{L^2}{E(v) \cdot R}\right)$. Accordingly, the link through-
 755 put T_0 for one pair of nodes can be computed as

$$T_0 = \frac{L_0}{I} = \Theta\left(\frac{R^2 B}{L^2}\right) \quad (31)$$

757 Meanwhile, R should be chosen on the order of $\Theta(L/\sqrt{n})$,
 758 i.e., $\frac{R}{L} = \Theta\left(\frac{1}{\sqrt{n}}\right)$ [8, 9]. Therefore, the above equation is
 759 reduced to $T_0 = \Theta(B/n) = \Theta(1/n)$. For each source node,
 760 except for the direct path, we can have at most $n - 2$ such 2-
 761 hop paths to help deliver its packet to destination. Therefore,
 762 the per source-destination throughput can be computed as

$$\Lambda(n) \leq T_0 \cdot (n - 2) \Rightarrow \Lambda(n) = \Theta(1). \quad (32)$$

764 Thus far, we have obtained exactly the same results in
 765 [8, 9] on throughput, and the above analysis leads to the
 766 following conclusion on the throughput $\Lambda(n)$ of a MANET
 767 subjected to the two-hop forwarding discipline.

768 **Theorem 1** For MANETs with unrestricted mobility, we
 769 have $\Lambda(n) = \Theta(1)$ for generic mobility models.

8.2 Delay & storage 770

771 To compute the delay and storage incurred in a MANET,
 772 we assume that every relay node maintains a separate
 773 queue for each S-D pair and the queue is served in a
 774 First-Come-First-Serve (FCFS) manner. Because all cells

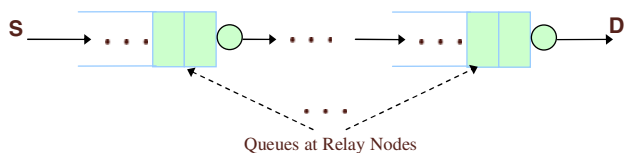


Fig. 14 Tandem queue

775 resemble each other and nodes have iid movements, it is
776 clear that all such queues are similar.

777 Consider an S-D queue at relay node m_r , a packet arrives
778 when node m_r and the previous relay node (or the source
779 node) simultaneously come into the communication region;
780 a packet departs when m_r meets another relay node (or the
781 destination node) in the communication region. Both the
782 inter-arrival time and the inter-departure time are of the
783 same order as link interarrival time (LIT) from the mobility
784 models in [21]. We also know from [21] that LIT can be
785 characterized as exponentially distributed, each queue is
786 then characterized of a Poisson arrival process with expo-
787 nential service time, thus being an M/M/1-FCFS queue.

788 For each S-D pair, queues at relay nodes construct a
789 M/M/1-FCFS feedforward tandem network⁴ as in Fig. 14.
790 An important property of a M/M/1-FCFS feedforward
791 tandem network is the *Jackson's theorem* (see [24], page
792 150), i.e., if the tandem network with exponential service
793 time is driven by a Poisson arrival process, every queue in
794 the tandem network behaves as if it were an independent
795 M/M/1-FCFS queue and thus can be analyzed individually.
796 Recall the following properties for a M/M/1-FCFS queue
797 (see [24], chapter 3) in the following lemma.

798 **Lemma 1** Consider a discrete M/M/1-FCFS queue. Let
799 $1 - \epsilon$ be the traffic intensity and λ be the exponential
800 service rate of the queue, the average delay is given by

$$E(D) = \frac{1}{\lambda\epsilon} = \Theta\left(\frac{1}{\lambda}\right) \tag{33}$$

802 Furthermore, the mean and variance of the occupancy of
803 the queue N_q is

$$E(N_q) = \frac{1 - \epsilon}{\epsilon} = \Theta(1) \tag{34}$$

$$805 \text{ } Var(N_q) = \frac{1 - \epsilon}{\epsilon^2} = \Theta(1) \tag{35}$$

807 Recall that the service rate of each queue can be written
808 as $\lambda = \Theta\left(\frac{E(v)R}{L^2}\right)$ [21] and also that the delay for each S-D
809 pair is the summation of delays occurred at relay nodes.
810 Assuming that every relay node carries traffic for $\Theta(n)$ S-D

4FL01 ⁴ For delay to be finite, the arrival rate must be strictly less than the
4FL02 service rate but in this case, symmetric movements lead to a fully
4FL03 loaded tandem queue. To avoid this, we assume that if the available
4FL04 throughput is $\Lambda(n)$, each source generates traffic at a rate $(1 - \epsilon)\Lambda(n)$,
4FL05 for some $\epsilon > 0$.

811 pairs, we can now summarize the network performance in
812 terms of average delay and storage in the following theorem.

813 **Theorem 2** The average packet delay in MANETs with
814 unrestricted mobility is given by

$$D(n) = \Theta\left(\frac{L^2}{E(v)R}\right) \tag{36}$$

and the average information bit delay $D_b(n)$ is 816

$$D_b(n) = \frac{D(n)}{L_0} = \Theta\left(\frac{L^2}{R^2B}\right) \tag{37}$$

Furthermore, the mean and variance of the packet
819 occupancy (i.e., storage requirement) is given by

$$E(N_p) = Var(N_p) = \Theta(n) \tag{38}$$

and the corresponding bit storage requirement N_b is 821

$$E(N_b) = Var(N_b) = \Theta(n) \cdot \Theta\left(\frac{RB}{E(v)}\right) \tag{39}$$

Summarizing, we can make the following observations: 823

- Throughput of the network scales as $\Lambda(n) = \Theta(1)$ and 824
packet-wise storage scales as $\Theta(n)$. Attaining optimal 825
throughput comes with the price of increase in storage. 826
- Mobility can help alleviate packet delay but it does not 827
help the bit-wise delay. It might be counter intuitive on 828
a first glance. However, a detailed examination reveals 829
that faster mobility brings more opportunities for nodes 830
to deliver information packets but at the cost of reduced 831
time for each communication. When information 832
packets are optimally chosen, the negative effect from 833
reduced communication time balances off the benefit 834
from faster mobility. Eventually, the only way to 835
reduce the bit-wise delay is to increase the bandwidth 836
and data rate for transmission, or use more transmission 837
power to increase the communication range. 838

9 Conclusions 840

841 We have presented an analytical framework for the char-
842 acterization of link and path lifetimes in MANETs with
843 unrestricted mobility. Given the existence of prior attempts
844 to incorporate link dynamics in the modeling of routing and
845 clustering schemes [4, 25, 26], we believe that this new
846 framework will find widespread use by researchers inter-
847 ested in the analytical modeling and optimization of MAC
848 and routing protocols in MANETs. The advantage of our
849 framework is that it accurately describes link and path
850 dynamics as a function of node mobility.

851 We illustrated how our framework can be applied by
852 using it to address the optimization of packet lengths and

853 the design of route caching strategies as a function of link
854 and path dynamics in MANETs. The optimized solutions
855 obtained from the proposed analytical framework show a
856 substantial improvement on network throughput and pro-
857 tocol performance. Furthermore, a performance analysis of
858 throughput, delay and storage is also presented for MA-
859 NETs using the two-hop forwarding scheme proposed by
860 Grossglauser & Tse [8, 9] to give deeper insights to the
861 understanding of system tradeoffs.

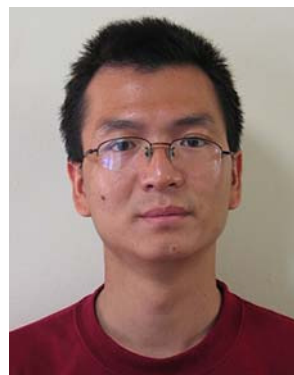
862 **Acknowledgements** The authors would like to thank Dr. Robin
863 Groenevelt and Prof. Philippe Nain of INRIA Institute for their kind
864 help on providing the simulation environment. This work was sup-
865 ported in part by the US Army Research Office under grants
866 W911NF-04-1-0224, W911NF-05-1-0246 and by the Baskin Chair of
867 Computer Engineering. Opinion, interpretations, conclusions and
868 recommendations are those of the authors and are not necessarily
869 endorsed by the Department of Defense.

870 References

- 871 1. Carvalho, M., & Garcia-Luna-Aceves, J. J. (2004, September). A
872 scalable model for channel access protocols in multihop ad hoc
873 networks. *Proceedings of the 10th annual international confer-
874 ence on Mobile computing and networking*, pp. 330–344.
- 875 2. Wu, L., & Varshney, P. (1999). Performance analysis of csma
876 and btma protocols in multihop networks (i) single channel case.
877 *Information Sciences—Informatics and Computer Science: An
878 International Journal*, 120, 159–177.
- 879 3. McDonald, A. B., & Znati, T. (1999, September). A path avail-
880 ability model for wireless ad-hoc networks. *Proceedings of IEEE
881 wireless communications and networking conference*, pp. 35–40.
- 882 4. Tsirigos, A., & Haas, Z. J. (2004). Analysis of multipath routing.
883 part i. The effect on the packet delivery ratio. *IEEE Transactions
884 on Wireless Communications*, 3(1), 138–146.
- 885 5. Samar, P., & Wicker, S. B. (2004, May). On the behavior of
886 communication links of a node in a multi-hop mobile environ-
887 ment. *Proceedings of the 5th ACM international symposium on
888 mobile ad hoc networking and computing*, pp. 148–156.
- 889 6. Samar, P., & Wicker, S. B. Link dynamics and protocol design in
890 a multi-hop mobile environment. *To appear In IEEE Transac-
891 tions on Mobile Computing*.
- 892 7. Wu, X., Sadjadpour, H. R., & Garcia-Luna-Aceves, J. J. (2007,
893 April). Link lifetime as a function of node mobility in manets
894 with restricted mobility: Modeling and applications. *Proceedings
895 of 5th international symposium on modeling and optimization in
896 mobile, ad hoc, and wireless networks*.
- 897 8. Grossglauser, M., & Tse, D. (2001, April). Mobility increases the
898 capacity of ad-hoc wireless network. *Proceedings of twentieth
899 annual joint conference of the IEEE computer and communica-
900 tions societies*, pp. 1360–1369.
- 901 9. Grossglauser, M., & Tse, D. (2002). Mobility increases the
902 capacity of adhoc wireless networks. *IEEE/ACM Transactions on
903 Networking*, 10(4), 477–486.
- 904 10. Gammal, A. E., Mammen, J., Prabhaker, B., & Shah, D. (2004,
905 March). Throughput-delay trade-off in wireless networks.
906 *Proceedings of IEEE INFOCOM*, pp. 464–475.
- 907 11. Le Boudec, J.-Y., & Vojnovic, M. (2006). The random trip
908 model: stability, stationary regime, and perfect simulation. *IEEE/
909 ACM Transactions on Networking*, 14(6), 1153–1166.

- 910 12. Jiang, S., He, D., & Rao, J. (2001, April). A prediction-based link
911 availability estimation for mobile ad hoc networks. *Proceedings
912 of IEEE INFOCOM*, pp. 1745–1752.
- 913 13. Jiang, S., He, D., & Rao, J. (2005). A prediction-based link
914 availability estimation for routing metrics in manets. *IEEE/ACM
915 Transactions on Networking*, 13(6), 1302–1312.
- 916 14. McDonald, A. B., & Znati, T. F. (1999). A mobility-based
917 framework for adaptive clustering in wireless ad hoc networks.
918 *IEEE Journal on Selected Areas in Communications*, 17(8),
919 1466–1487.
- 920 15. Bettstetter, C. (2001). Mobility modeling in wireless network:
921 categorization, smooth movement and border effects. *ACM
922 Mobile Computing and Communication Review*, 5, 55–67.
- 923 16. Guerin, R. (1987). Channel occupancy time distribution in a
924 cellular ratio system. *IEEE Trans. on Vehicular Technology*,
925 35(3), 89–99.
- 926 17. Bansal, N., & Liu, Z. (2003, April). Capacity, delay and mobility
927 in wireless ad-hoc networks. *Proceedings of IEEE INFOCOM*,
928 pp. 1553–1563.
- 929 18. Hong, D., & Rappaport, S. S. (1986). Traffic model and perfor-
930 mance analysis for cellular mobile radio telephone systems with
931 prioritized and non prioritized handoff procedures. *IEEE Trans-
932 actions on Vehicular Technology*, 35(3), 77–92.
- 933 19. Han, Y., La, R. J. (2006, April). Path selection in mobile ad-hoc
934 networks and distribution of path duration. *Proceedings of IEEE
935 INFOCOM*, pp. 1–12.
- 936 20. Han, Y., La, R. J., Makowski, A. M., & Lee, S. (2006). Distri-
937 bution of path durations in mobile ad-hoc networks: Palm's
938 theorem to the rescue. *Computer Networks*, 50(12), 1887–1900.
- 939 21. Groenevelt, R., Koole, G., & Nain, P. (2005). Message delay
940 in mobile ad hoc networks. *Performance Evaluation*, 62,
941 210–228.
- 942 22. Perkins, C. E., & Royer, E. M. (1999, February). Ad hoc on-demand
943 distance vector routing. *Proceedings of the 2nd IEEE workshop on
944 mobile computing systems and applications*, pp. 90–100.
- 945 23. Johnson, D., Hu, Y., & Maltz, D. (2004). The dynamic source
946 routing protocol for mobile ad hoc networks (dsr). Internet Draft,
947 draft-ietf-manet-dsr-10.txt, IETF MANET Working Group.
- 948 24. Kleinrock, L. (1975). *Queueing Systems, Volume 1: Theory*. John
949 Wiley & Sons, Inc.
- 950 25. Sadagopan, N., Bai, F., Krishnamachari, B., & Helmy, A. (2003,
951 June). Paths: Analysis of path duration statistics and their impact
952 on reactive manet routing protocols. *Proceedings of the 4th ACM
953 international symposium on mobile adhoc networking and com-
954 puting*, pp. 245–256.
- 955 26. Turgut, D., Das, S., & Chatterjee, M. (2001, May). Longevity of
956 routes in mobile ad hoc networks. *Proceedings of vehicular
957 technology conference*, pp. 2833–2837.

Author Biographies



960 **Xianren Wu** received the B.S.
961 Degree in Communication
962 Engineering from Nanjing
963 University of Posts and Tele-
964 communications, Nanjing,
965 China, in 1998 and the M.S.
966 degree in information engineer-
967 ing from Beijing University of
968 Posts and Telecommunications,
969 Beijing, China, in 2001. He is
970 currently a Ph.D. candidate at
971 University of California at Santa
972 Cruz, with research topic on
973 analytical modeling and
974

975
976
977
978

performance analysis of mobile ad hoc networks. And he received best paper award in SPECTS 2007 conference. His general research interest spans over mobile ad hoc networks, wireless communications and coding theory.

981
982
983
984
985
986
987
988
989
990
991
992
993
994
995
996
997
998
999
1000
1001
1002
1003
1004
1005
1006
1007
1008
1009
1010
1011
1012
1013

Hamid R. Sadjadpour received his B.S. and M.S. degrees from Sharif University of Technology with high honor and Ph.D. degree from University of Southern California in 1986, 1988, and 1996 respectively. After graduation, he joined AT&T as a member of technical staff, later senior technical staff member, and finally Principal member of technical staff at AT&T Lab. in Florham Park, NJ until 2001. In fall 2001, he joined University

of California, Santa Cruz (UCSC) where he is now an Associate professor. He has served as technical program committee member in numerous conferences and as chair of communication theory symposium at WirelessCom 2005, and chair of communication and information theory symposium at IWCMC 2006, 2007, and 2008 conferences. He has been also Guest editor of EURASIP on special issue on Multicarrier Communications and Signal Processing in 2003 and special issue on Mobile Ad Hoc Networks in 2006, and is currently Associate editor for Journal of Communications and Networks (JCN). He has published more than 90 publications. His research interests include space-time signal processing, scaling laws for wireless ad hoc networks, performance analysis of ad hoc and sensor networks, and MAC layer protocols for MANETs. He is the co-recipient of International Symposium on Performance Evaluation of Computer and Telecommunication Systems (SPECTS) 2007 best paper award. He holds more than 13 patents, one of them accepted in spectrum management of T1.E1.4 standard.



J. J. Garcia-Luna-Aceves holds the Jack Baskin Chair of Computer Engineering at the University of California, Santa Cruz (UCSC), and is a Principal Scientist at the Palo Alto Research Center (PARC). Prior to joining UCSC in 1993, he was a Center Director at SRI International (SRI) in Menlo Park, California. He has been a Visiting Professor at Sun Laboratories and a Principal of Protocol Design at Nokia. Dr. Garcia-Luna-Aceves has published a book, more than 330

papers, and 24 U.S. patents. He has directed 25 Ph.D. theses and 20 M.S. theses since he joined UCSC in 1993. He has been the General Chair of the IEEE SECON 2005 Conference; Program Co-Chair of ACM MobiHoc 2002 and ACM Mobicom 2000; Chair of the ACM SIG Multimedia; General Chair of ACM Multimedia '93 and ACM SIGCOMM '88; and Program Chair of IEEE MULTIMEDIA '92, ACM SIGCOMM '87, and ACM SIGCOMM '86. He has served in the IEEE Internet Technology Award Committee, the IEEE Richard W. Hamming Medal Committee, and the National Research Council Panel on Digitization and Communications Science of the Army Research Laboratory Technical Assessment Board. He has been on the editorial boards of the IEEE/ACM Transactions on Networking, the Multimedia Systems Journal, and the Journal of High Speed Networks. He is a Fellow of the IEEE and is listed in Marquis Who's Who in America and Who's Who in The World. He is the co-recipient of Best Paper Awards at the IEEE MASS 2007, SPECTS 2007, IFIP Networking 2007, and IEEE MASS 2005 conferences, and the Best Student Paper Award of the 1998 IEEE International Conference on Systems, Man, and Cybernetics. He received the SRI International Exceptional-Achievement Award in 1985 for his work on multimedia communication and in 1989 for his work on routing algorithms.

1014
1015
1016
1017
1018
1019
1020
1021
1022
1023
1024
1025
1026
1027
1028
1029
1030
1031
1032
1033
1034
1035
1036
1037
1038
1039
1040
1041
1042
1043
1044
1045
1046
1047
1048
1049
1050
1051
1052
10531054
1055